Effect of Fluid Motion on the Aggregation of Small Particles Subject to Interaction Forces

Stefano Melis, Marcel Verduyn, Giuseppe Storti, and Massimo Morbidelli
ETH Zürich, Laboratorium für Technische Chemie LTC, Universitätstrasse 6, CH-8092 Zürich, Switzerland

Jerzy Bałdyga
Dept. of Chemical and Process Engineering, Warsaw University of Technology, 00-645 Warsaw, Poland

The effect of bulk fluid motion on aggregation of small particles subject to interaction forces of the DVLO type is investigated. In particular, the convection-diffusion equation for the probability of finding two particles at a given relative position is solved numerically for the case of an axisymmetrical linear flow field, which approximates a turbulent flow field. The effect of bulk motion is shown to be important particularly in the case of thick double layers, where a critical size exists above which aggregation exhibits a self-accelerating behavior, that is, the aggregation rate constant increases with particle size. On the other hand, systems with thin double layers appear to be almost unaffected by shear. An approximate criterion for distinguishing between these two cases is presented.

Introduction

Aggregation of solid particles dispersed in a fluid medium is important in a wide variety of processes such as precipitation, crystallization, and emulsion polymerization, since it affects the particle-size distribution of the final product. Typically, the evolution of the particle-size distribution is modeled through a population balance equation (PBE) (Ramkrishna, 1985). This is usually written using particle mass as internal coordinate, to which particle size can be related assuming some particle shape, for example, spherical. In the case of a purely aggregating system (that is, without breakup and particle growth) in a homogeneous vessel with constant volume, the relevant PBE can be written as follows

$$\frac{\partial f(m,t)}{\partial t} = -f(m,t)\int_0^\infty \beta(m,m',t)f(m',t)\,dm' + \frac{1}{2}\int_0^m \beta(m-m',m',t)f(m-m',t)f(m',t)\,dm' \quad (1)$$

where $f(m,t)$ is the number density of particles of mass m at time t, and β is the rate constant for aggregation, which depends on the size (and, in general, on the shape) of the two colliding particles, as well as on the operating conditions. Its evaluation requires the development of appropriate physical models, which describe in detail the aggregation process. This can be done by considering a pair of particles and calculating the probability of finding these two particles in a given relative position, that is, the pair probability function (van de Ven, 1989). For this, a balance equation is used which accounts for the main mechanisms affecting the relative motion of the two particles, that is, Brownian diffusion, transport by fluid motion, and interparticle forces. External forces are not considered and particle inertia is neglected. The latter assumption is justified for the small particles (no larger than few microns) considered in this work. From the pair probability function, the aggregation rate constant β can be computed as the flux across a properly selected collision surface.

Due to the complexity of this problem, two cases are typically considered in the literature, where particle aggregation is dominated by Brownian diffusion (perikinetic) or by transport due to fluid motion (orthokinetic).

Perikinetic aggregation

The simplest case, where aggregation of noninteracting particles occurs by Brownian diffusion only, usually referred to as the fast aggregation limit, was solved in the classical work by Smoluchowski (1917), leading to the following ex-

Correspondence concerning this article should be addressed to M. Morbidelli.

pression for the aggregation rate constant β between two spherical particles of radii a_1 and a_2

$$\beta = 4\pi\,\mathfrak{D}_0(a_1 + a_2) = 8\pi\,\mathfrak{D}_0 a \tag{2}$$

where a indicates a characteristic particle dimension, assumed equal to the arithmetic mean of the radii of the two colliding particles, and $\mathfrak{D}_0$ is the mutual diffusion coefficient, given by

$$\mathfrak{D}_0 = \frac{kT}{6\pi\mu}\left(\frac{1}{a_1} + \frac{1}{a_2}\right) = \frac{kT}{6\pi\mu}\,\frac{(1+\lambda)^2}{2a\lambda} \tag{3}$$

where μ is the viscosity of the dispersing medium and λ is the particle size ratio a_2/a_1.

When interparticle forces are considered, β is given by the Smoluchowski relation 2 divided by the Fuchs' stability ratio W. Its expression, in the general form derived by Spielman (1970), is given by

$$W = 2\int_2^\infty \frac{\exp(V/kT)}{G(\xi,\lambda)\,\xi^2}\,d\xi \tag{4}$$

where V is the potential energy of the interparticle forces, $\xi = r/a$ is the center-to-center dimensionless distance, and $G(\xi,\lambda)$ accounts for the additional resistance caused by the squeezing of the fluid between the two approaching particles.

Orthokinetic aggregation

The case where aggregation is dominated by convection, that is, the particles are transported by movement of the surrounding fluid, was first analyzed by Smoluchowski (1917), who considered noninteracting particles in a shear flow field undisturbed by the particles themselves. The analysis was extended to a turbulent flow field by Saffman and Turner (1956). They assumed that particles smaller than the smallest eddies move like in a shear flow, whose rate of shear is related to the rate of energy dissipation through the Taylor microscale relations. In both cases it was found that the aggregation rate constant is proportional to the rate of shear E and the cube of the particle characteristic dimension a through a proportionality constant α, which depends on the type of shear field considered (such as extensional, 1-D simple shear, and so on)

$$\beta = \alpha a^3 E \tag{5}$$

This result can be improved by accounting for the effect of the particles on the flow field. In the case of particles with significantly different sizes, it is reasonable to account for the modification in the flow field induced by the larger particle only (Pneuli et al., 1991). Further refinements, that is, accounting for the disturbance of the flow field by both particles, lead to vanishing values of the aggregation rate constant, since the approaching particle velocity becomes equal to zero at the collision surface (van de Ven and Mason, 1976). This corresponds to the fact that at small distances the aggregation behavior is governed not by convection but rather by the short distance interaction forces, such as van der Waals attractive forces. In more general terms, this problem has been solved by considering DLVO type interparticle potentials, which account not only for the van der Waals contribution, but also for electrostatic repulsive forces (Verwey and Overbeek, 1948). This problem was addressed by van de Ven and Mason (1976), Zeichner and Schowalter (1997), and Adler (1981a,b) who developed a detailed analysis of the particle trajectories and computed numerically the aggregation rate. Of course, when electrostatic repulsive forces are dominant, this approach leads to vanishing values of the aggregation rate constant.

Intermediate regimes of aggregation

The full problem, where all three mechanisms for particle motion are included, was considered by Zeichner and Schowalter (1977), van de Ven and Mason (1977), and Feke and Schowalter (1983, 1985). The former, following Swift and Friedlander (1964), obtained the overall aggregation rate as the sum of the contributions due to perikinetic and orthokinetic aggregation evaluated separately. Van de Ven and Mason (1977) developed a perturbation analysis of the relevant pair probability equation with respect to a parameter representing the ratio between the convective and the diffusive terms, that is, the Peclet number Pe. It was found that shear enhances the aggregation rate and that this enhancement is proportional to the square root of the Peclet number. Therefore, the perikinetic and orthokinetic contributions are not directly additive. This analysis was limited to very small values of Pe. The high Peclet number limit was treated by Feke and Schowalter (1983, 1985) who expanded the same pair probability equation with respect to the inverse of the Peclet number. Their conclusion was that Brownian motion can either enhance or hinder shear induced aggregation, depending upon the specific operating conditions. More recently, the collision of drops in simple shear flow at arbitrary Pe, with van der Waals attraction but without repulsive forces, has been analyzed by Zinchenko and Davis (1995).

From the earlier discussion, it appears that the behavior of aggregating systems is well understood in the limiting situations where either the peri- or the orthokinetic mechanism dominates. On the other hand, the behavior of these systems is not well understood in the transition regime, where all mechanisms for particle aggregation contribute significantly. In this work, in order to investigate the system behavior under such conditions, the pair probability equation for a system of two spherical particles subject to interaction forces of DLVO type, embedded in an extensional flow field, is solved numerically. This kind of flow field was selected because it well reproduces the structure of turbulent flow below the scale of the smallest eddies (Batchelor, 1980), that is, at the scale relevant for the motion of the small particles of interest in this work. Although the developed model can account for heterocoagulation, simulation results are shown only for equal-sized particles, since also in this case the essential features of aggregating systems are well evident. In the following, after discussing the main features of the developed aggregation model, the behavior of the aggregation rate constant is examined for various intensities of the fluid turbulence, that is, the extension rate, and of the particle inter-

action forces. The obtained results are then compared with those obtained with the limiting models discussed above in order to investigate the transition of the aggregating system between the peri- and the orthokinetic mechanism.

Two Particle Aggregation Model

A system of two small spherical particles of radii a_1 and a_2 in a fluid medium is considered. As mentioned above, these particles are transported by the fluid, diffuse by Brownian motion and are subject to interaction forces, while inertial forces can be neglected. This last assumption holds when the particle Reynolds number is much smaller than unity, which in practice corresponds to analyzing particles smaller than few microns for the extensional flow field considered in the following or, when referring to a turbulent flow field, to particles smaller than the Kolmogorov scale η defined as

$$\eta = \left(\frac{\nu^3}{\epsilon}\right)^{1/4} \tag{6}$$

where ϵ is the rate of energy dissipation of the flow field and ν is the kinematic viscosity. For such a system, the pair probability function c is governed by the following convection-diffusion equation

$$\frac{\partial c}{\partial t} = \nabla\cdot\left(D\nabla c - \boldsymbol{v}_{\text{int}}c - \boldsymbol{v}_f c\right) \tag{7}$$

where D is the diffusion tensor, while $\boldsymbol{v}_{\text{int}}$ and $\boldsymbol{v}_f$ are convective terms representing the effect of interparticle forces and transport by fluid motion, respectively.

In terms of dimensionless interparticle, the associated boundary conditions (BCs) are given by

$$c = 0 \quad \text{at} \quad \xi = 2; \quad c = 1 \quad \text{at} \quad \xi = \infty \tag{8}$$

which state that the two particles aggregate when they reach a distance $r = a_1 + a_2$, that is, $c = 0$ at $\xi = 2$, and that bulk conditions prevail when the two particles are at infinite separation. The aggregation rate constant can be computed by integrating the particle flux over the entire collision surface S, represented by a sphere of radius $(a_1 + a_2)$, as follows

$$\beta = \int_S \left(D\nabla c - \boldsymbol{v}_{\text{int}}c - \boldsymbol{v}_f c\right)\cdot n\, dS \tag{9}$$

where n is the normal to the collision surface.

It is worth noting that in general dynamics of the relative motion of the two particles, described by Eq. 7, is much faster than the dynamics of the evolution of the particle size population, described for example by Eq. 1. In other words, Eq. 7 attains pseudo-steady-state conditions with respect to both the population balance equation and the vortex lifetime. Therefore, in the following only the steady-state solution of Eq. 7 and the corresponding steady-state value for β are considered. Before this, the evaluation of the two velocities $\boldsymbol{v}_f$ and $\boldsymbol{v}_{\text{int}}$ are discussed in detail.

Particle transport by bulk fluid motion (Batchelor and Green, 1972)

According to Kolmogorov theory of turbulence (Hinze, 1975) at scales smaller than the Kolmogorov microscale defined by Eq. 6, the flow is governed by viscous phenomena. Therefore, this system can be described by considering two particles embedded in a linear flow field. Furthermore, Batchelor (1979) indicated that a turbulent flow can be effectively represented by assuming an axisymmetrical extensional flow. With these two positions, the components of the relative particle velocity $\boldsymbol{v}_f$ in spherical coordinates are given by (Batchelor and Green, 1972)

$$v_{f,r} = \frac{1}{2}Ea\xi\left[1 - A(\xi,\lambda)\right](3\cos^2\theta - 1) \tag{10}$$

$$v_{f,\theta} = -\frac{3}{2}Ea\xi\left[1 - B(\xi,\lambda)\right]\sin\theta\cos\theta \tag{11}$$

where θ is the polar angle, while the azimuthal velocity component vanishes. A bidimensional representation of these trajectories is shown in Figure 1. The functions $A(\xi,\lambda)$ and $B(\xi,\lambda)$ account for the effect of the presence of the particles on the fluid motion. Rigorous expressions for these functions are not available except for $\lambda \to 0$. Approximate expressions are available for $\lambda > 0$ in terms of asymptotic expansions for the near and the far field only (Kim and Karrila, 1991). To have a single expression for the whole field, algebraic expressions interpolating the numerical results reported by Batchelor and Green (1972) for $\lambda = 1$ have been used in this work, as reported in the Appendix.

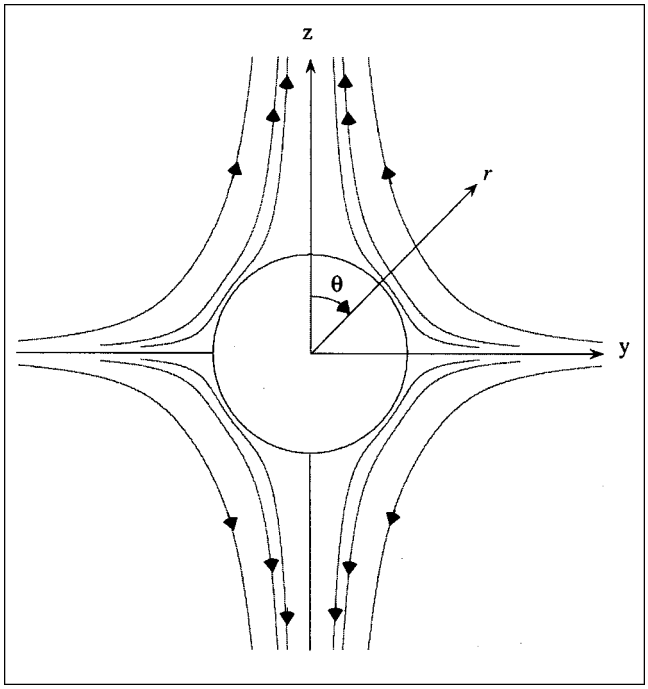

Figure 1. Relative velocity of two particles embedded in an axisymmetrical extensional flow field.

In the previous equations E indicates the rate of extension, which is a function of the rate of energy dissipation ϵ. For a locally homogeneous and isotropic turbulent flow field, the mean value of E is given by (Batchelor, 1953)

$$\langle E \rangle = \frac{7}{6\sqrt{15}} S \sqrt{\frac{\epsilon}{\nu}} \tag{12}$$

where S is a skewness factor for the distribution of E, usually set equal to 0.6. Since only extensional fields which simulate turbulent conditions are considered, only positive values of E are considered in the following. It is worth noting that Eq. 12 provides only a local average value. This agrees with the Kolmogorov theory, but neglects the distribution of E resulting from the intermittent, fine-scale properties of turbulence. In other terms, the model could be improved by integrating the aggregation rate over the spectrum of shear rates characteristic of a given turbulent field.

Motion induced by interparticle forces

Colloidal interactions are usually described through the DLVO theory (Verwey and Overbeek, 1948), which accounts for van der Waals and electrostatic forces. The overall DLVO potential V is given by the sum of an attractive (V_A) and a repulsive (V_R) contribution.

The scaled potential energy $\psi_A = V_A/kT$ due to van der Waals forces for two spherical particles is expressed by the Hamaker relation (Israelachvili, 1991)

$$\psi_A(\xi) = -\frac{Ha}{6}\left[\frac{8\lambda}{(1+\lambda)^2}\left(\frac{1}{\xi^2-4}+\frac{1}{\xi^2-4\Lambda^2}\right) + \ln\left(\frac{\xi^2-4}{\xi^2-4\Lambda^2}\right)\right] \tag{13}$$

where Ha represents the dimensionless Hamaker constant, defined as the ratio between the Hamaker constant A and the scaling factor kT, and $\Lambda = (1-\lambda)/(1+\lambda)$. Corrections to Eq. 13 were introduced by Schenkel and Kitchener (1960), who accounted for retardation effects caused by the finite speed of light. However, in the frame of this modeling analysis, such corrections are not applied.

About the scaled potential energy of repulsion $\psi_R = V_R/kT$, electrostatic forces arise when particles are electrically charged. In this case, the particles are surrounded by ions of opposite sign, forming an electrical double layer, where the distribution of counterions is given by the Poisson-Boltzmann equation. When two equally charged particles approach each other, their double layers overlap, leading to a repulsive force between the two particles (van de Ven, 1989). A rigorous treatment of this system is very difficult, since it involves the simultaneous solution of the Poisson-Boltzmann equation along with the convection-diffusion equation for each ionic species and integration of the resulting stresses over the particle surfaces. For small and constant surface potentials (that is, particles approaching each other sufficiently slow to maintain electrostatic equilibrium) and using Derjaguin approximation (Derjaguin, 1934, 1989), Hogg, Healy and Fürstenau (1966) developed the following relationship

$$\psi_R(\xi) = 2\pi N_R Ha \frac{\lambda}{(1+\lambda)^2}(1+\Phi^2) \times \left\{\frac{2\Phi}{1+\Phi^2}\ln\left[\frac{1+\exp[-\kappa a(\xi-2)]}{1-\exp[-\kappa a(\xi-2)]}\right] + \ln\{1-\exp[-2\kappa a(\xi-2)]\}\right\} \tag{14}$$

where $\Phi = \phi_{s2}/\phi_{s1}$ is the ratio between the surface potentials, N_R expresses the importance of the repulsive forces relative to the attractive ones (Zeichner and Schowalter, 1977), and κ is the Debye-Hückel constant. The last two quantities are defined as follows

$$N_R = \frac{\chi \phi_{s1}^2 a}{A}; \qquad \kappa = \sqrt{2\frac{e^2 I_s N_A}{\chi kT}} \tag{15}$$

where I_s indicates the ionic strength and χ the dielectric constant of the medium. Strictly speaking, Eq. 14 applies only to small surface potentials and thin double layers (that is, $\kappa a > 1$). Although more rigorous expressions were developed by Papadopoulos and Cheh (1984) and by Ohshima and coworkers (1983, 1994), in this analysis Eq. 14 was retained also for κa values close to unity.

A typical behavior of the overall potential energy as a function of dimensionless particle separation is shown in Figure 2, where three cases, corresponding to unstable, moderately stable and stable systems, are illustrated.

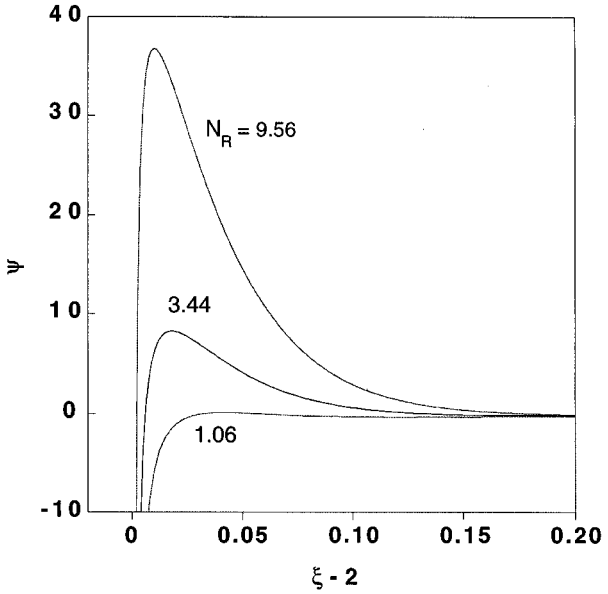

Figure 2. Potential energy of interaction for a stable ($N_R = 9.56$), a moderately stable ($N_R = 3.44$), and an unstable system ($N_R = 1.06$).

Parameter values: $a = 100$ nm; $\lambda = 1$; $\Phi = 1$; $\kappa a = 10.4$.

The particle interaction force is obtained by taking the gradient of the overall interaction potential $\psi = \psi_A + \psi_R$. Since this is a function of the interparticle distance only, ξ (see Eqs. 13 and 14), the resulting force is directed along the line of centers. From this, the induced velocity is evaluated as follows (Batchelor, 1976)

$$\boldsymbol{v}_{\text{int}} = \frac{F_{\text{int}}}{6\pi\mu}\frac{(1+\lambda)^2}{2a\lambda}G(\xi,\lambda) = -\mathfrak{D}_0\nabla\psi\, G(\xi,\lambda) \quad (16)$$

where $G(\xi,\lambda)$ is given as an infinite series (Spielman, 1970). In this work the approximate expression developed by Honig et al. (1971) for $\lambda = 1$, was used as reported in the Appendix.

Motion induced by Brownian diffusion

The diffusion term is treated here following Batchelor (1976), who determined the hydrodynamic corrections to the diffusion coefficient supposing the existence of a fictitious Brownian force which acts on both particles with the same magnitude, but with opposite direction. This leads to the following expressions for the radial and polar components of the diffusion tensor

$$\mathfrak{D}_r = \mathfrak{D}_0 G(\xi,\lambda); \qquad \mathfrak{D}_\theta = \mathfrak{D}_0 H(\xi,\lambda) \quad (17)$$

Since, as discussed below, tangential diffusion will not be considered in the computations carried out in this article, the form of the function $H(\xi,\lambda)$ is not specified.

Resulting equation and numerical solution

By rewriting Eq. 7 in spherical coordinates, at steady state, and using the expressions derived in the previous paragraphs, the following equation is obtained

$$\frac{2}{Pe}\frac{1}{\xi^2}\frac{\partial}{\partial\xi}\left[\xi^2 G(\xi,\lambda)\left(\frac{\partial c}{\partial\xi} + c\frac{\partial\psi}{\partial\xi}\right)\right] - \frac{(3\cos^2\theta - 1)}{\xi^2}\frac{\partial}{\partial\xi}\{c\xi^3[1 - A(\xi,\lambda)]\} + 3\frac{(1 - B(\xi,\lambda))}{\sin\theta}\frac{\partial}{\partial\theta}(c\sin^2\theta\cos\theta) = 0 \quad (18)$$

where the Peclet number $Pe = Ea^2/\mathfrak{D}_0$ has been introduced and BCs 8 apply. Since most of the computations reported in the following section are characterized by values of the Peclet number larger than unity, in the above equation the tangential diffusion has been neglected. This is not the case for the radial diffusion, which is larger due to the additional contribution of the velocity induced by the interaction forces. In cases where a Peclet number close to unity was considered, it was verified numerically that the tangential term $[1/(a^2\xi^2\sin\theta)(\partial/\partial\theta)][\sin\theta\,\mathfrak{D}_\theta(\partial c/\partial\theta)]$ is negligible with respect to the radial one $[(1/a^2\xi^2)(\partial/\partial\xi)][\xi^2\mathfrak{D}_r(\partial c/\partial\xi)]$ close to the collision surface, while the convective term prevails at large interparticle separations. The negligibility of tangential diffusion is furthermore supported by the findings of Zinchenko and Davis (1994) for the case of drop coalescence. Their results indicate that tangential diffusion contributes to the aggregation rate by 2–3% only in the case of small *Pe* and becomes completely negligible for *Pe* exceeding 5.

The algorithm developed to solve Eq. 18 consists of a first step where the equation is solved along the radial direction at $\theta = \pi/2$. Here, since $v_{f,\theta}$ vanishes, Eq. 18 reduces to a second-order ordinary differential equation which is solved by discretizing in the radial direction using central finite differences and solving the resulting system of linear algebraic equations through the routine DLSARB (IMSL Fortran Numerical Libraries). Note that the integration field is divided into two subdomains, one very narrow ($2 < \xi \le 3$) close to the collision surface where interparticle forces are significant and where the discretization grid is rather fine (that is, $\Delta\xi = 5\times10^{-4}$), and the other one for the remaining part of the domain, where a coarser discretization grid is used (that is, $\Delta\xi = 1\times10^{-2}$).

The obtained solution provides the initial condition for the second step which consists in integrating Eq. 18 in the tangential direction. In this case, the Gear method (routine DIVPAG, IMSL Fortran Numerical Libraries) is used. Convergence of the algorithm is verified using an integral criterion, that is, verifying that the computed flux β (Eq. 9) through various surfaces enclosing the reference particle is constant.

With respect to the application of the BCs (8), a maximum separation of 15 to 30 times the reference particle radius has been considered. In addition, equiprobability of the pair probability function (that is, $c = 1$) was imposed only in the part of the boundary where the flux is incoming (upstream), while the remaining part of the boundary (downstream) is treated as an open one, that is, imposing continuity of pair probability and flux across the boundary.

A final remark concerns the limitations of the numerical algorithm, which exhibits convergence difficulties for values of the Debye-Hückel parameter larger than 5×10^8 m^{-1}. For this case, the double layer forces act over an extremely short range and, therefore, the discretization procedure fails.

Results and Discussion

The behavior of the aggregation rate constant computed through Eq. 9 is analyzed, using the pair probability function *c* given by Eq. 18 as a function of the Peclet number for various values of particle sizes, ionic strength, and surface potentials, while in all cases constant values of the following quantities have been used: dimensionless Hamaker constant $Ha = 1.58$ (corresponding to the case of polystyrene particles in aqueous solution), fluid viscosity $\mu = 10^{-3}$ Pa·s, fluid kinematic viscosity $\nu = 10^{-6}$ m^2·s^{-1}, dielectric constant $\chi = 6.91\times10^{-10}$C^2·m^{-2}·N^{-1}, and temperature $T = 298$ K. The obtained results are compared with the predictions of the limiting models discussed in the previous section for pure peri- and orthokinetic aggregation.

Coupling between diffusive and convective aggregation mechanisms

The first case considered refers to relatively large particles ($a = 100$ nm; $\lambda = 1$) and unstable conditions, that is, small electrostatic forces ($N_R = 0.27$, $\Phi = 1$, and $\kappa a = 33.0$). In Fig-

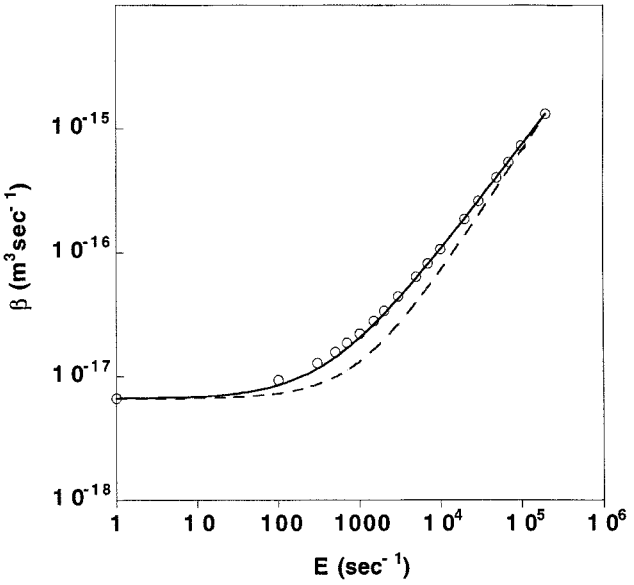

Figure 3. Aggregation rate constant, β as a function of extension rate, E for a fast aggregating system.

Parameter values: $a = 100$ nm; $\lambda = 1$; $N_R = 0.27$; $\Phi = 1$; $\kappa a = 33.0$. Rigorous model (○); Eq. 20 (——); Eq. 21 (– – –).

ure 3 it is seen that for small values of the extension rate, E the aggregation rate computed by the rigorous model (circles) approaches the pure perikinetic limit, where Eq. 4 holds. On the other hand, in the limit of large E values, β varies nonlinearly with E, thus in disagreement with the Smoluchowski analysis (Eq. 5). Actually, by fitting the rigorous model results in the limit of large E values, the following empirical expression is obtained

$$\beta = \gamma E^{0.86} \tag{19}$$

Note that the value of the exponent of E (0.86) coincides with the one obtained by Zeichner and Schowalter (1977) through a trajectory analysis. Using this expression for the evaluation of the limiting convective value of β and adopting the assumption of flux additivity (Swift and Friedlander, 1964)

$$\beta = \beta_{\text{diff}} + \beta_{\text{conv}} = \frac{8\pi \mathcal{D}_0 a}{W} + \gamma E^{0.86} \tag{20}$$

the continuous curve in Figure 3 is obtained. The good agreement with the results of the rigorous model indicates that the diffusive and convective mechanisms can be considered independent of each other for unstable systems. For a comparison, in Figure 3, the results obtained by applying the flux additivity assumption and evaluating β_{conv} through Eq. 5

$$\beta = \beta_{\text{diff}} + \beta_{\text{conv}} = \frac{8\pi \mathcal{D}_0 a}{W} + \alpha a^3 E \tag{21}$$

are also shown. It is seen that even in this simple case the predictions given by this relation are rather poor.

The picture changes completely when considering more stable systems, that is, with larger electrostatic forces, as the one shown in Figure 4 ($a = 100$ nm, $\lambda = 1$, $N_R = 2.39$, $\Phi = 1$ and $\kappa a = 10.4$). For this case, the aggregation rate vs. E curve exhibits a sigmoidal shape which approaches the same limits as in the previous case, that is, β_{diff} for $E \to 0$ and β_{conv} given by Eq. 19 for $E \to \infty$. However, for this system, the additivity assumption (Eq. 20) leads to the values shown by the continuous line in Figure 4 which exhibit large discrepancies from the results of the rigorous model. Somehow better results are obtained with the flux additivity assumption, when β_{conv} is computed more accurately, that is, by directly solving the following equation

$$\frac{1}{\xi}\frac{\xi}{\partial \xi}\left[\xi^2 (\upsilon_{\text{int}} + \upsilon_{f,r}) c\right] + \frac{1}{\sin\theta}\frac{\partial}{\partial \theta}\left(\upsilon_{f,\theta} c \sin\theta\right) = 0 \tag{22}$$

which is equivalent to Eq. 18 except for the diffusion term, which is here neglected. The obtained results (dashed line in Figure 4) differ again significantly from those of the rigorous model, particularly in the region where the transition from perikinetic to orthokinetic aggregation occurs. This indicates that, for slowly aggregating systems, the diffusive and the convective aggregation mechanisms interact with each other, and, therefore, the flux additivity assumption is not valid. In conclusion, the two simplified models above can only be regarded as upper and lower bounds for the aggregation rate constant and, therefore, can be used only for extreme values of the extension rate.

Finally, an example of calculated pair probability function is shown in Figure 5 for three different values of the angle θ. An overshoot is evident in all examined cases, that is, the

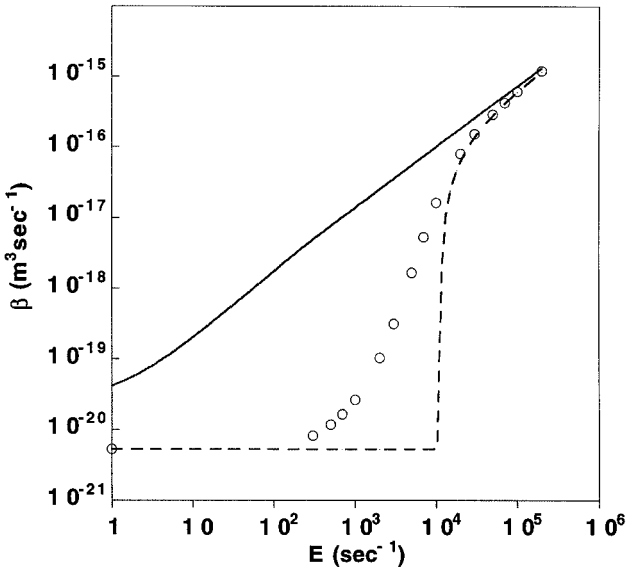

Figure 4. Aggregation rate constant, β as a function of extension rate, E for a slow aggregating system.

Parameter values: $a = 100$ nm; $\lambda = 1$; $N_R = 2.39$; $\Phi = 1$; $\kappa a = 10.4$. Rigorous model (○); Eq. 20 (——); trajectory analysis + diffusive contribution (– – –).

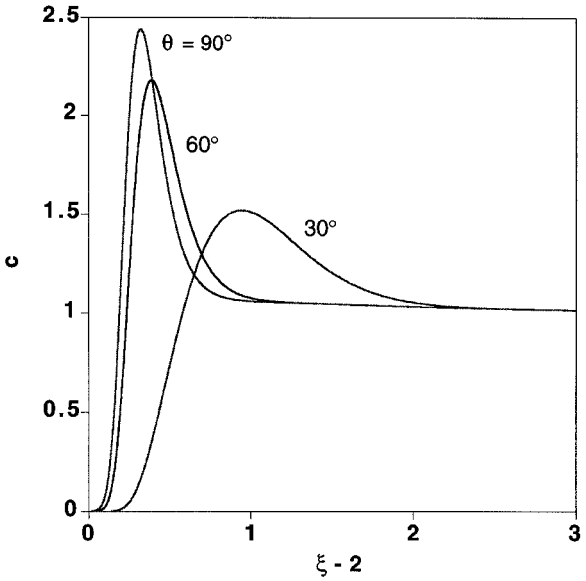

Figure 5. Steady-state pair probability function, c as a function of dimensionless particle separation, ξ at three different values of the polar angle θ.

Parameter values: $a = 100$ nm; $\lambda = 1$; $N_R = 2.39$; $\Phi = 1$; $\kappa a = 10.4$; $Pe = 4.58$.

pair probability close to the reference particle becomes larger than that at infinite distance. This apparently singular behavior is the result of the interaction between convection and diffusion, as previously described in the literature (Feke and Schowalter, 1983; Zinchenko and Davis, 1994).

Effect of ionic strength

The effect of ionic strength is analyzed in Figures 6a and 6b, where the interparticle DLVO potential and the corresponding aggregation rate constant are shown for various values of the ionic strength ($a = 100$ nm, $\lambda = 1$, $N_R = 2.39$, $\Phi = 1$ and $\kappa a = 4.7$, 10.4, and 33.0, respectively). In agreement with the perikinetic limit, in Figure 6b it is seen that for small values of the extension rate, increasing values of the ionic strength lead to larger values of the aggregation rate. On the other hand, the behavior is reversed at larger values of E. This can be qualitatively justified by considering that a decrease in the ionic strength leads to a smaller value of the Debye-Hückel parameter (see Eq. 15), which, in turn, implies both an increase in magnitude of the potential energy maximum, as well as its shift towards larger values of interparticle separation, as shown in Figure 6a. The overall effect in the case of a stagnant fluid is simply the increase of the stability ratio, which leads to a decrease of the aggregation rate constant. On the other hand, when convection is significant, it is possible that even when the potential energy barrier is higher, the probability that an incoming particle can surpass it can be still higher, since, at larger separations, the particles have a larger relative velocity. Therefore, the decreased ionic strength may lead to larger aggregation rates. Finally, at very high E values, ionic strength does not play any role, since the velocity induced by interaction forces becomes negligible with respect to that induced by the bulk fluid motion, and, in fact, all curves in Figure 6b approach the same asymptote given by Eq. 19 as $E \to \infty$.

The discussion above leads to the conclusion that, at least for the conditions investigated in this work, the aggregation rate is more strongly affected by fluid motion in the case of thick double layers, that is, for low values of ionic strength.

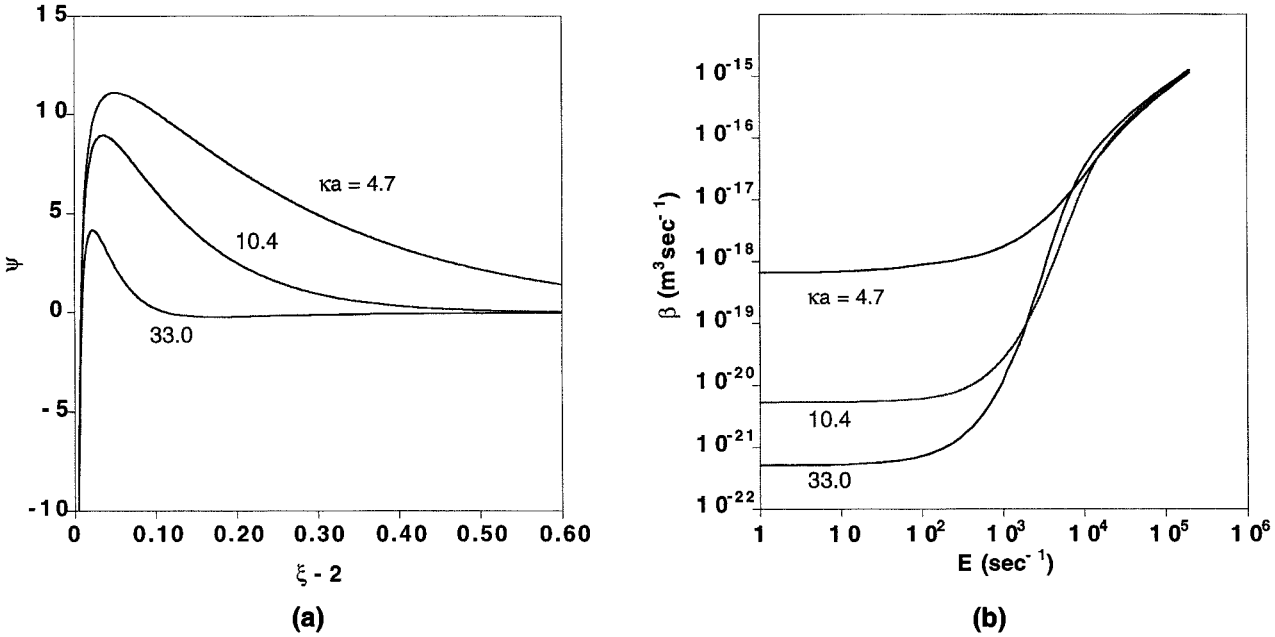

Figure 6. (a) Scaled potential energy of interaction ψ as a function of dimensionless particle separation ξ; (b) aggregation rate constant β as a function of extension rate E for different values of κa.

Parameter values: $a = 100$ nm; $\lambda = 1$; $N_R = 2.39$; $\Phi = 1$.

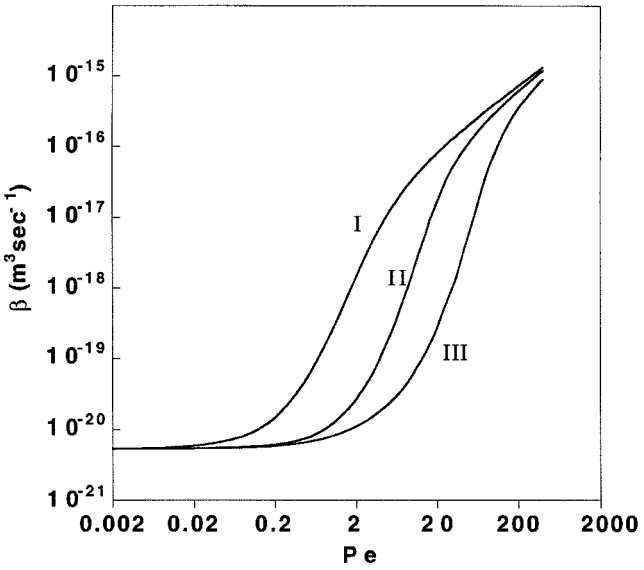

Figure 7. Aggregation rate constant β as a function of Peclet number *Pe* for three systems at constant value of the stability ratio *W*.

(I) $N_R = 1.53$; $\kappa a = 1.2$; (II) $N_R = 2.39$; $\kappa a = 10.4$; (III) $N_R = 4.25$; $\kappa a = 44$. Parameter values: $a = 100$ nm; $\lambda = 1$; $\Phi = 1$.

This is further demonstrated in Figure 7, where the aggregation rate constant values for three different operating conditions are compared as a function of the Peclet number, $Pe = Ea^2/\mathfrak{D}_0$. Different values of both ionic strength (corresponding to $\kappa a = 1.2$, 10.4 and 44.0) and surface potentials (corresponding to $N_R = 1.53$, 2.39 and 4.25, with $\Phi = 1$ always) were selected in order to obtain in each case the same value of the stability ratio $W = 3{,}868$, but different values of the double layer thickness. For case II, a significant deviation from the pure Brownian aggregation occurs when the Peclet number equals 2, corresponding to an approximate fivefold increase in the aggregation rate constant. On the other hand, for case III at the same *Pe* value, the aggregation rate increases only by a factor two and we have to increase the Peclet number up to 6 in order to have a comparable fivefold increase in the aggregation rate constant. In case I, the fluid motion has a very strong effect, so that at $Pe = 2$, the aggregation is already close to the limiting orthokinetic mechanism. Under these conditions, the aggregation rate constant is 300 times larger than the value corresponding to Brownian aggregation.

As expected, the Peclet number does not identify uniquely the situation where convection starts to be important. From Figure 7, it is seen that, depending on the intensity of the interparticle forces, the *Pe* value, where convection starts to play a role, changes by about two orders of magnitude. Since it is convenient in applications to have an easy criterion to establish whether or not the aggregation rate is affected by fluid dynamics, a modified Peclet number is introduced. This is done noting that there are two characteristic lengths involved in this process. In the case of a thin double layer ($\kappa a > 1$), the diffusion flux is proportional to $\mathfrak{D}_0/L$, where the characteristic length $L = 1/\kappa$ is equal to the thickness of the double layer. On the other hand, the convective flux is proportional to the radial velocity $v_{f,r}$ which can be estimated from Eq. 10 at a particle distance $a + 1/\kappa$. Thus, the following expression for the modified Peclet number $\overline{Pe}$ is obtained

$$\overline{Pe} = \frac{E(a + 1/\kappa)}{\kappa\, \mathfrak{D}_0} = Pe \frac{1 + \kappa a}{(\kappa a)^2} \tag{23}$$

It is readily seen that with this new definition, $\overline{Pe}$ is equal to the classical Peclet number multiplied by a correction factor. This quantity, being a function of the dimensionless distance of the potential energy maximum from the particle surface, $1/\kappa a$, reflects the interparticle interactions. It can be seen that, when such a distance decreases and *Pe* is constant, the value of $\overline{Pe}$ decreases, thus indicating that the extension rate *E* should be increased in order for the convective mechanism to affect the aggregation rate. This is coherent with the observation that the radial fluid velocity is lower closer to the particle surface and, therefore, the convective contribution to aggregation is smaller. The conclusion that $\overline{Pe}$ provides a better indication on whether the aggregation rate is affected by fluid dynamics is given in Figure 8, where the same values of the aggregation rate constant, as in Figure 7, are plotted as a function of the modified Peclet number $\overline{Pe}$. It is seen that in this case the three curves are brought much closer to each other, and that the value $\overline{Pe} = 1$ is well-centered in the middle of the transition from peri- to orthokinetic aggregation regime. This result suggests $\overline{Pe} > 0.1$ as a general criterion for the aggregation rate to be dependent on system fluid dynamics. Finally, note that in this representation the asymptotic behavior of the three curves for large $\overline{Pe}$ values is not coincident anymore, as it was in Figure 7. This is due to the fact that interparticle forces do not affect the coagulation phenomenon at such large values of Peclet number so that the correction factor does not apply.

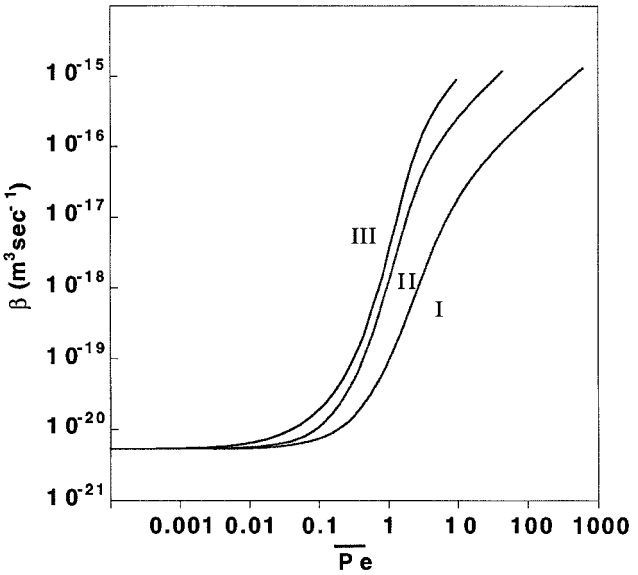

Figure 8. Aggregation rate constant β as a function of the modified Peclet number $\overline{Pe}$ for three systems at constant value of the stability ratio *W*.

Parameter values as in Figure 7.

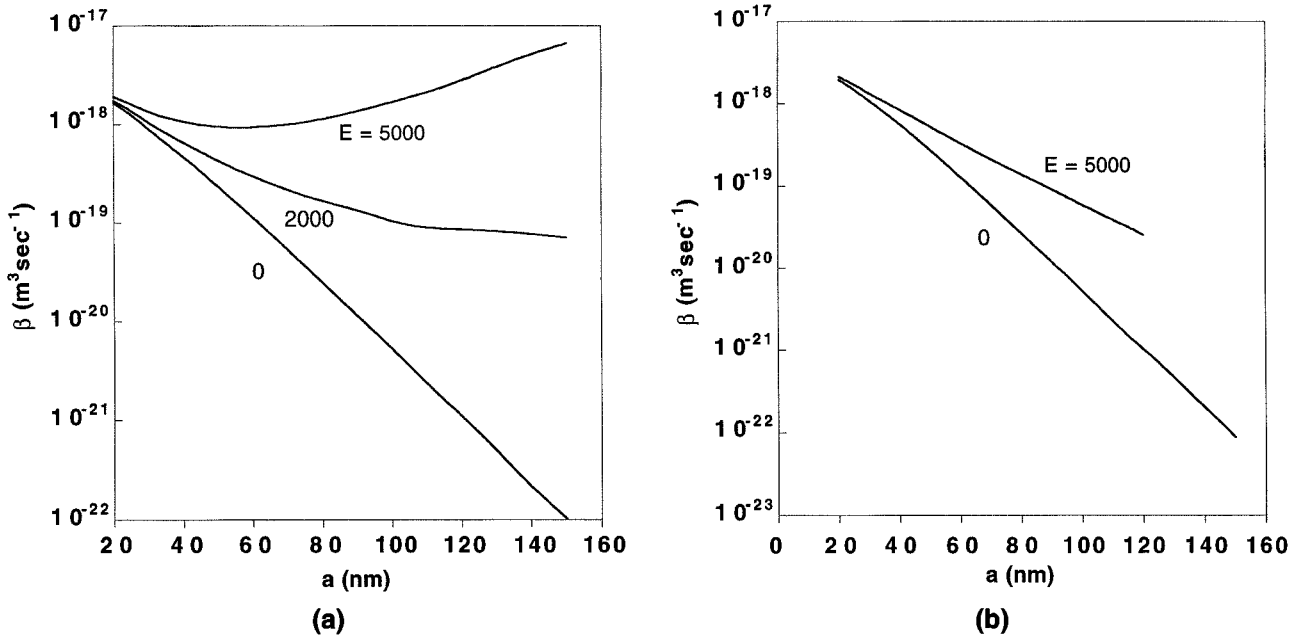

Figure 9. Aggregation rate constant β as a function of particle size a ($\lambda = 1$) for different values of the extension rate E (s^{-1}), and for thick (a) and thin (b) double layer.

Parameter values: (a) $N_R/a = 2.39\times10^{-7}$ m^{-1}; $\Phi = 1$; $\kappa = 1.04\times10^{8}$ m^{-1} and (b) $N_R/a = 4.25\times10^{-7}$ m^{-1}; $\Phi = 1$; $\kappa = 4.40\times10^{8}$ m^{-1}.

Effect of particle size

The behavior of the aggregation rate constant as a function of particle size for various values of the extension rate is now considered. For this case, the results in terms of dimensional variables are presented in order to give a better reference to measurable quantities. The case of a moderately thick double layer ($N_R/a = 2.39\times10^{-7}$ m^{-1}, $\Phi = 1$, $\kappa = 1.04\times10^{8}$ m^{-1}) is illustrated in Figure 9a, where the model results for $E = 0$, 2,000 and 5,000 s^{-1} are shown. The aggregation rate constant decreases as particle size increases in the case of moderate rates of extension. On the other hand, at larger extension rates, the curves exhibit a minimum which shifts towards smaller values of particle radii for larger values of the extension rate. This behavior can be explained by considering that, as the particle size increases, the potential energy of repulsion increases, thus making aggregation less likely. This effect dominates for low rates of extension, and, in fact, in Figure 9a for $E = 0$, the value of β decreases continuously as particle size increases. For larger values of the extension rate, the convective mechanism of aggregation becomes more important, particularly for large particles. As can be seen in Figure 9a, for sufficiently large particle sizes, the aggregation rate constant increases with particle size, and this occurs the sooner the larger the value of E. Note that the particle size value where this phenomenon occurs, which corresponds to the location of the minimum in the curve with $E > 0$, can be regarded as a critical particle size, since beyond this value particle aggregation is favored for larger particles. This may explain the formation of few and very large pieces of coagulum often encountered in applications. An approximate estimation of such a critical size can be obtained from the modified Peclet number defined in Eq. 23. For example, in the case of $E = 5{,}000$ s^{-1} shown in Figure 9a, the critical particle size is about 50 nm, which corresponds to a modified Peclet number close to unity: $\overline{Pe} = 1.25$.

However, since the aggregation of particles with thin double layers is only slightly sensitive to fluid motion, it follows that the curves in Figure 9b ($N_R/a = 4.25\times10^{-7}$ m^{-1}, $\Phi = 1$, $\kappa = 4.40\times10^{8}$ m^{-1}) exhibit a monotonously decreasing behavior. Note that this result is in good agreement with the criterion developed in the previous section to find out the effect of fluid dynamics on particle aggregation. The calculated values of the modified Peclet number ($\overline{Pe} = 0.4$ for the larger size considered, that is, 120 nm) indicate a moderate effect of fluid dynamics, so that the presence of a minimum in the aggregation rate constant for $\overline{Pe}$ around 1 is not expected.

Conclusion

In this work, the effect of hydrodynamics on the aggregation of small particles subject to interaction forces of DLVO type was investigated theoretically. For this, the steady-state convection-diffusion equation was developed and solved, expressing the pair probability as a function of relative position for a two particle system embedded in an extensional flow field. Such a flow field was chosen in order to best simulate the turbulent conditions for particles having diameters smaller than the Kolmogorov scale. From the solution of this equation, it is possible to compute the aggregation rate constant, which is the key input parameter used in population balance equations to compute the time evolution of the PSD in aggregating systems.

Several simulations were performed to investigate the effect of various operating parameters of interest in applications such as particle size, ionic strength and mixing intensity

on the aggregation rate constant. In all cases it was found that the results of the rigorous model approach the limits of peri- and orthokinetic aggregation, as described by simpler models previously developed in the literature, for very small and very large values of the Peclet number, respectively. However, in general, only the rigorous model results are available for intermediate values. In particular, for fast aggregating systems it has been shown that the diffusive and convective contributions to the aggregation rate are independent, so that the additivity assumption for the fluxes can be used to calculate the overall aggregation rate for intermediate values of the extension rate. On the other hand, more stable systems exhibit a strong nonlinear coupling between convection and diffusion which causes the flux additivity assumption to fail.

The performed simulations allow to conclude that the effect of hydrodynamics is more pronounced in the case of long-range electrostatic forces, that is, when the ionic strength is low and, therefore, the double layer is thick. Consequently, for these systems, large increases in the magnitude of the aggregation rate constant are possible even when the Peclet number is rather small. On the other hand, stable systems characterized by thin double layers seem to exhibit weak sensitivity to fluid bulk motion. In order to provide a quick, approximate criterion for determining whether or not fluid dynamics affects the aggregation rate, a modified expression of the Peclet number $\overline{Pe}$ was introduced (see Eq. 23), which accounts to a certain extent for the presence of interparticle forces. For all simulations reported in this work, it was found that the condition $\overline{Pe} < 0.1$ allows to exclude all those operating conditions where fluid dynamics affects aggregation.

Another result of this analysis is that fluid motion can strongly affect the aggregation of very small particles, whose behavior instead often in the literature is considered to be independent of shear. In particular, it is found that for relatively large extension rates, the aggregation rate constant exhibits a minimum when plotted against particle size. This indicates the existence of a critical particle size, above which the aggregation rate constant becomes larger for larger particles, thus leading to some kind of ''runaway'' of the aggregation phenomenon, which would lead to few but very large pieces of coagulum, such as those often encountered in applications. It is shown that this behavior is not exhibited by systems with a thin double layer.

Acknowledgments

We gratefully acknowledge the financial support by the Swiss National Science Foundation (grant NF 2100-50504).

Notation

a = reference particle radius, $= (a_1 + a_2)/2$
a_i = radius of particle i
$A(r, \lambda)$ = hydrodynamic function for radial velocity (cf. Appendix)
$B(r, \lambda)$ = hydrodynamic function for tangential velocity (cf. Appendix)
e = charge of electron
F_{int} = interaction force
$G(r, \lambda)$ = hydrodynamic function for radial diffusion (cf. Appendix)
$H(r, \lambda)$ = hydrodynamic function for tangential diffusion
m = particle mass
N_A = Avogadro number
r = radial coordinate
t = time
T = temperature
α = constant of proportionality (Eq. 5)
γ = constant of proportionality (Eq. 19)
η = Kolmogorov scale (Eq. 6)
ϕ_s = surface potential
ψ = interaction potential energy
ψ_R = repulsive interaction potential energy

Subscripts and superscripts

0 = bulk conditions
r = radial direction
θ = tangential direction

Literature Cited

Adler, P. M., ''Heterocoagulation in Shear Flow,'' *J. Coll. Int. Sci.*, **83**, 106 (1981a).
Adler, P. M., ''Interaction of Unequal Spheres. I. Hydrodynamic Interaction: Colloidal Forces,'' *J. Coll. Int. Sci.*, **84**, 461 (1981b).
Batchelor, G. K., *The Theory of Homogeneous Turbulence*, Cambridge University Press, Cambridge (1953).
Batchelor, G. K., ''Brownian Diffusion of Particles with Hydrodynamic Interaction,'' *J. Fluid Mech.*, **74**, 1 (1976).
Batchelor, G. K., ''Mass Transfer from a Particle Suspended in Fluid with a Steady Linear Ambient Velocity Distribution,'' *J. Fluid Mech.*, **95**, 369 (1979).
Batchelor, G. K., ''Mass Transfer from Small Particles Suspended in Turbulent Fluid,'' *J. Fluid Mech.*, **98**, 609 (1980).
Batchelor, G. K., and J. T. Green, ''The Hydrodynamic Interaction of Two Small Freely-Moving Spheres in a Linear Flow Field,'' *J. Fluid Mech.*, **56**, 375 (1972).
Derjaguin, B. V., ''Untersuchungen über die Reibung und Adhesion, IV. Theorie des Anhaftens kleiner Teilchen,'' *Kolloid Z.*, **69**, 155 (1934).
Derjaguin, B. V., *Theory of Stability of Colloids and Thin Films*, Consultants Bureau, New York and London (1989).
Feke, D. L., and W. R. Schowalter, ''The Effect of Brownian Diffusion on Shear-Induced Coagulation of Colloidal Dispersions,'' *J. Fluid Mech.*, **133**, 17 (1983).
Feke, D. L., and W. R. Schowalter, ''The Influence of Brownian Diffusion on Binary Flow-Induced Collision Rates in Colloidal Dispersions,'' *J. Coll. Int. Sci.*, **106**, 203 (1985).
Hinze, J. O., *Turbulence*, McGraw-Hill, New York (1975).
Hogg, R., T. W. Healy, and D. W. Fürstenau, ''Mutual Coagulation of Colloidal Dispersions,'' *Trans. Faraday Soc.*, **62**, 1638 (1966).
Honig, E. P., G. J. Roebersen, and P. H. Wiersema, ''Effect of Hydrodynamic Interaction on the Coagulation Rate of Hydrophobic Colloids,'' *J. Coll. Int. Sci.*, **36**, 97 (1971).
Israelachvili, J., *Intermolecular & Surface Forces*, Academic Press, London (1991).
Kim, S., and S. Karrila, *Microhydrodynamics*, Butterworth-Heinemann, Boston (1991).
Ohshima, H., D. Y. C. Chan, T. W. Healy, and L. R. White, ''Improvement on the Hogg-Healy-Fürstenau Formulas for the Interaction of Dissimilar Double Layers,'' *J. Coll. Int. Sci.*, **92**, 232 (1983).
Ohshima, H., ''Electrostatic Interaction between Two Dissimilar Spheres: An Explicit Analytic Expression,'' *J. Coll. Int. Sci.*, **162**, 487 (1994).
Papadopoulos, K. D., and H. Y. Cheh, ''Theory on Colloidal Double-Layer Interactions,'' *AIChE J.*, **30**, 7 (1984).
Pnueli, D., C. Gutfinger, and M. Fichman, ''A Turbulent-Brownian Model for Aerosol Coagulation,'' *Aerosol Sci. Technol.*, **14**, 201 (1991).
Ramkrishna, D., ''The Status of Population Balances,'' *Rev. Chem. Eng.*, **31**, 435 (1985).
Saffman, P. G., and J. S. Turner, ''On the Collision of Drops in Turbulent Clouds,'' *J. Fluid Mech.*, **1**, 16 (1956).
Schenkel, J. H., and J. A. Kitchener, ''A Test of the Derjaguin-Verwey-Overbeek Theory with a Colloidal Suspension,'' *Trans. Faraday Soc.*, **56**, 161 (1960).
Smoluchowski, M., ''Versuch einer Mathematischen Theorie der Koagulations-Kinetik Kolloider Lösungen,'' *Z. Phys. Chem.*, **92**, 129 (1917).

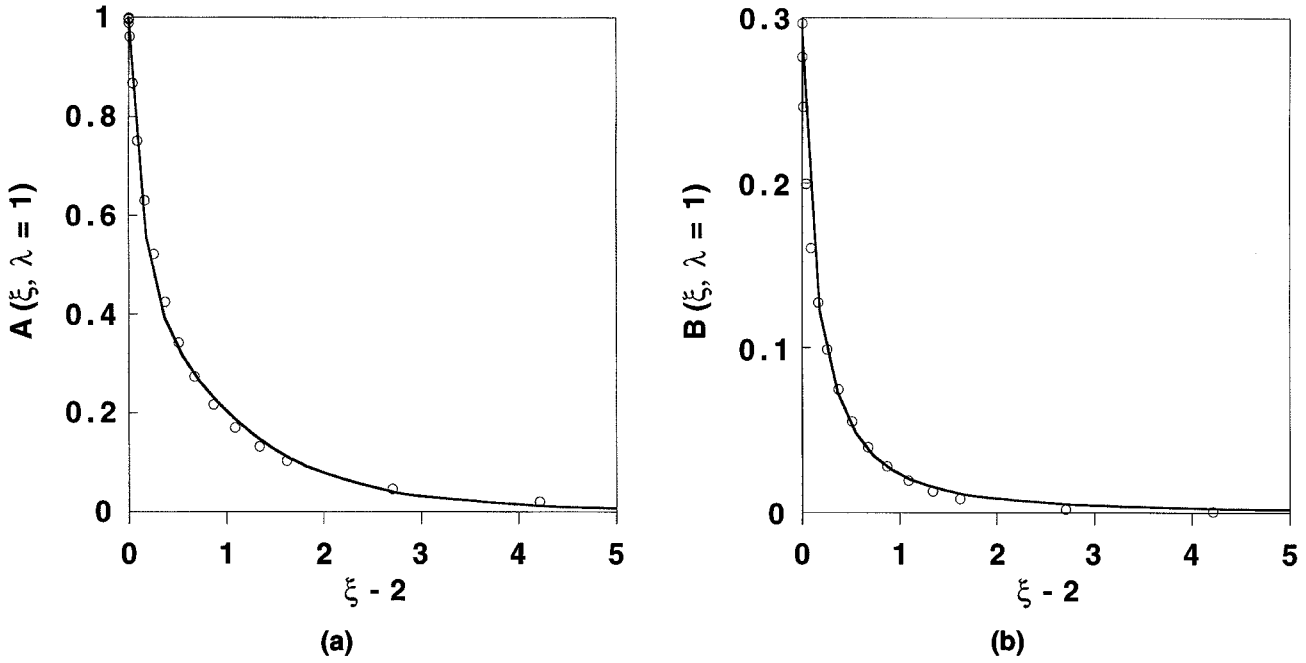

Figure 10. Hydrodynamic interaction functions (a) $A(\xi, \lambda = 1)$ and (b) $B(\xi, \lambda = 1)$ as a function of dimensionless particle separation ξ.

Equation A1 (——); numerical values after Batchelor and Green (1972) (○).

Spielman, L. A., "Viscous Interactions in Brownian Coagulation," *J. Coll. Int. Sci.*, **33**, 562 (1970).

Swift, D. L., and S. K. Friedlander, "The Coagulation of Hydrosols by Brownian Motion and Laminar Shear Flow," *J. Coll. Sci.*, **19**, 621 (1964).

van de Ven, T. G. M., *Colloidal Hydrodynamics*, Academic Press, London (1989).

van de Ven, T. G. M., and S. G. Mason, "The Microrheology of Colloidal Dispersions. IV. Pairs of Interacting Spheres in Shear Flow," *J. Coll. Int. Sci.*, **57**, 505 (1976).

van de Ven, T. G. M., and S. G. Mason, "The Microrheology of Colloidal Dispersions. VIII. Effect of Shear on Perikinetic Doublet Formation," *Coll. Polym. Sci.*, **255**, 794 (1977).

Verwey, E. J. W., and J. T. G. Overbeek, *Theory of the Stability of Lyophobic Colloids*, Elsevier, Amsterdam (1948).

Zeichner, G. R., and Schowalter, W. R., "Use of Trajectory Analysis to Study Stability of Colloidal Dispersions in Flow Fields," *AIChE J.*, **23**, 243 (1977).

Zinchenko, A. Z., and R. H. Davis, "Gravity Induced Coalescence of Drops at Arbitrary Peclet Numbers," *J. Fluid Mech.*, **280**, 119 (1994).

Zinchenko, A. Z., and R. H. Davis, "Collision Rates of Spherical Drops or Particles in a Shear Flow at Arbitrary Peclet Numbers," *Phys. Fluids*, **7**, 2310 (1995).

Table 1. Numerical Values of the Coefficients in Eq. A1

Hydrodynamic Function $A(\xi, \lambda = 1)$			
i	a_i		
1	113.2568893		
2	307.8264828		
3	−2,607.54064288		
4	3,333.72020041		
Hydrodynamic Function $B(\xi, \lambda = 1)$			
i	b_i	c_i	d_i
1	0.96337157	1.90461683	−1.99517070
2	−0.93850774	1.90378420	2.01254004

Appendix

Batchelor and Green (1972) solved numerically the equation of motion for two equal-sized spherical particles in a linear flow field. The obtained values of the hydrodynamic interaction functions $A(\xi, \lambda = 1)$ and $B(\xi, \lambda = 1)$ have been interpolated through the following algebraic expressions

$$A(\xi, \lambda = 1) = \sum_{i=1}^{4} \frac{a_i}{\xi^{i+4}}; \qquad B(\xi, \lambda = 1) = \sum_{i=1}^{2} \frac{b_i}{(\xi - c_i)^{d_i}} \tag{A1}$$

The numerical values of the coefficients a_i to d_i are summarized in Table 1. The agreement between the numerical values reported by Batchelor and Green (1972) and those calculated through Eq. A1 is shown in Figures 10a and 10b. Note that, for the hydrodynamic function B, a good agreement is observed also at small gaps between the two particles, where an abrupt change takes place.

Following Honig et al. (1971), the following expression applies to the evaluation of the hydrodynamic function $G(\xi, \lambda)$ for equal sized particles

$$G(\xi, \lambda = 1) = \frac{6h^2 + 4h}{6h^2 + 13h + 2} \tag{A2}$$

where $h = \xi - 2$.

Manuscript received Aug. 5, 1998, and revision received Mar. 30, 1999.